Transformation Mechanism between High-Quartz and Keatite Phases of LiAlSi$_2$O$_6$ Composition*

By Chi-Tang Li

Owens-Illinois Technical Center, Toledo, Ohio, U.S.A.

The high-quartz phase of LiAlSi$_2$O$_6$ composition reconstructively transforms into the keatite phase at elevated temperature. The transformation matrix was first derived from the powder data and then confirmed by the single-crystal data. (Si,Al)-tetrahedra form 6- and 8-membered rings in the high-quartz phase but form 5-,7-, and 8-membered rings in the keatite phase. All the 6-membered rings and half of the 8-membered rings transform into 5- and 7-membered rings or a combination of both types of rings of the keatite phase. The linkages of other half of the 8-membered rings remain unchanged throughout the transformation. Transformation starts when either one common edge of two neighboring 6-membered rings is broken or the two adjacent edges, one at each ring, of the particular common edge are broken. During the transformation, most atoms undergo no change in linkage and little change in position. Two (Si,Al) atoms which break away from the old framework undergo a displacement of 2·6 Å, while the displacements of the remaining ten (Si,Al) atoms range only from 0·01 to 0·35 Å. This transformation study seems to indicate the possibility that the movement of each atom during the transformation may be followed by the use of the structural information.

Introduction

A stuffed high-quartz phase can be obtained by heat-treating a glass of spodumene composition LiAlSi$_2$O$_6$(Li$_2$O . Al$_2$O$_3$. 4SiO$_2$). The high-quartz phase transforms reconstructively into a stuffed keatite phase upon raising the heat-treatment temperature or time.

The crystal structures of both phases of LiAlSi$_2$O$_6$ composition at room temperature were solved by Li (1968) and Li & Peacor (1968). The structural data for both phases are briefly summarized in Table 1. The two structures are illustrated in Figs. 1, 2 and 3 where only (Si, Al) atoms are shown for the sake of clarity. This transformation study represents an attempt of trying to follow the movement of each atom during the transformation by using the room temperature structural data before and after the transformation. High

Table 1. *A summary of structural data for high-quartz and keatite phases of* LiAlSi$_2$O$_6$ *composition*

	Keatite solid solution	High-quartz solid solution
Space group	$P4_32_12$	$P6_222$
a (Å)	7·541	5·217
c (Å)	9·156	5·464
V (Å^3)	520·7	128·8
Z	4 (LiAlSi$_2$O$_6$)	1 (LiAlSi$_2$O$_6$)
Atomic parameters ($\times 10^3$)		
(Si, Al)	(8b) 332, 122, 238	(3c) 500, 0, 0
	(4a) 418, 418, 0	—
O	(8b) 443, 121, 393	(6j) 206, 412, 0
	(8b) 125, 116, 299	—
	(8b) 364, 305, 146	—
Li	(8b) 071, 195, 501	(3a) 0, 0, 0
Site-occupancy		
(Si, Al)	1	1
O	1	1
Li	$\frac{1}{2}$	$\frac{1}{3}$
Coordination No.		
(Si, Al)	4	4
Li	4	4
O	2 or 3	2 or 3
Loop of (Si, Al)-tetrahedra	5, 7 or 8	6 or 8
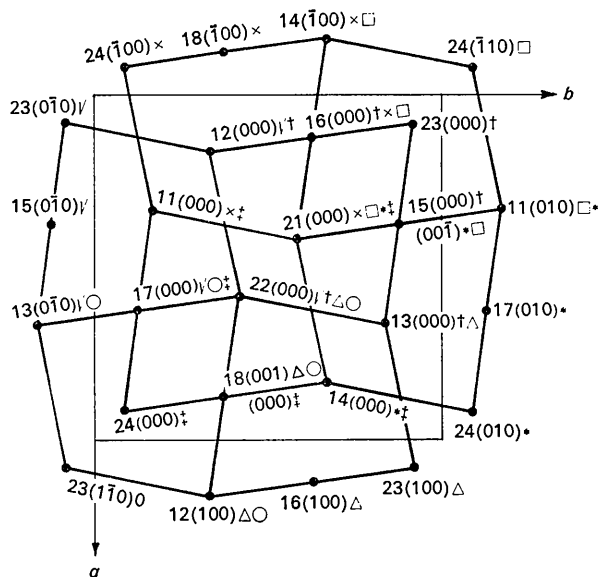
Fig. 1. The projection of LiAlSi$_2$O$_6$ high-quartz phase down the c axis of the equivalent keatite cell (The eight 6-membered rings are separately marked).
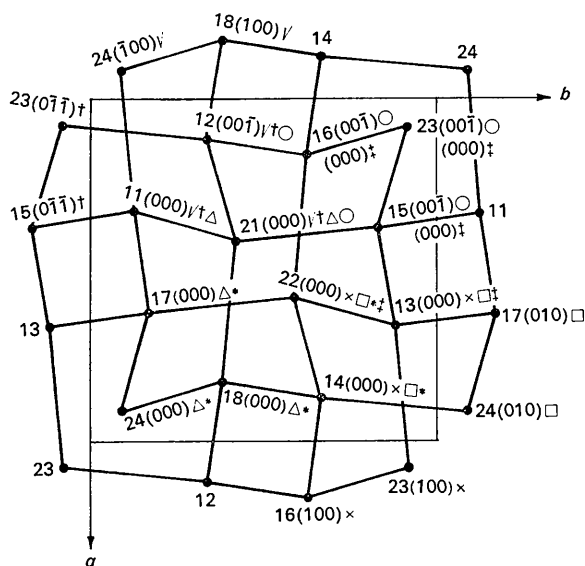
Fig. 2. The projection of LiAlSi$_2$O$_6$ keatite phase down the c axis (The eight 5-membered rings are separately marked).

temperature structural data and those of other elaborated methods are needed in order to confirm the findings in this study. However, according to the DTA analysis, the exothermal peak at the transformation point is very very small indeed when compared with that of glass crystallization. This observation tends to support the finding that most atoms undergo small positional changes. A very preliminary study of the transformation mechanism was made by Evans (1969) who indicated that a model of four high-quartz hexagonal cells (in orthorhombic axes) revealed fourfold screw distribution of tetrahedra.

Derivation of transformation matrix

High-quartz and keatite phases of LiAlSi$_2$O$_6$ composition can be related to each other by working out a matrix defining the unit-cell transformation. This transformation matrix can correlate index, lattice, and coordinate matrices in the following way:

$$\mathbf{h}(Q)=\mathbf{n}\mathbf{H}(K), \quad \mathbf{a}(Q)=\mathbf{n}\mathbf{A}(K), \quad \mathbf{x}(Q)=(\mathbf{n}^T)^{-1}\mathbf{X}(K)$$

where $\mathbf{n}^T$ and $\mathbf{n}^{-1}$ are the transpose and inverse of the transformation matrix $\mathbf{n}$. Those of the high-quartz phase are represented by h, a, x, and parenthetic Q, while H, A, X and parenthetic K are used to designate those of the keatite phase.

Only three independent pairs of equivalent reflections between high-quartz and keatite phases are required for the solution of the transformation matrix $\mathbf{n}$. The powder patterns of these two phases are very similar. From the powder data, three separate pairs of reflections having nearly equal interplanar spacings were chosen, as are listed in Table 2. They were found to be independent of one another, and the transformation matrix $\mathbf{n}$ was thus solved as follows:

$$\mathbf{n}=\begin{bmatrix} \frac{1}{4} & \frac{1}{4} & \frac{1}{2} \\ \frac{1}{4} & \frac{1}{4} & -\frac{1}{2} \\ \frac{1}{2} & -\frac{1}{2} & 0 \end{bmatrix} \qquad \mathbf{n}^{-1}=\begin{bmatrix} 1 & 1 & 1 \\ 1 & 1 & -1 \\ 1 & -1 & 0 \end{bmatrix}$$

Single-crystal data were used to confirm the solution of the matrix $\mathbf{n}$. According to the transformation matrix, the axes [100], [010], and [001] of the high-quartz phase correspond to the axes of [111], [11$\bar{1}$], and [1$\bar{1}$0] of the keatite phase, respectively. A single crystal of the keatite phase was mounted first on [111] and then on [1$\bar{1}$0] axes, and the corresponding photographs were taken. By the use of the index of each equivalent reflec-

Table 2. *A match of three pairs of powder reflections between high-quartz and keatite phases of* LiAlSi$_2$O$_6$ *composition*

	High-quartz phase				Keatite phase		
hkl	2θ*	*d*	I_1/I_0†	*HKL*	2θ*	*d*	I_1/I_0†
100	19·65°	4·518 Å	11·7	111	19·26°	4·608 Å	8·3
101	25·58	3·482	100·0	201	25·55	3·486	100·0
112	48·24	1·887	19·1	400	48·27	1·885	10·0

* Cu-radiation was used.
† The calculated integrated powder intensity was used.

tion pair, the transformation matrix **n** has been confirmed.

Applications of transformation matrix

Index matrix

Each independent high-quartz reflection transforms into one, two or three corresponding independent keatite reflections, depending on the symmetry of each particular reflection. On the other hand, each independent keatite reflection may be generated by one or two independent high-quartz reflections. Some of the index transformations are listed in Table 3.

Lattice matrix

A hexagonal lattice cannot exactly transform geometrically into a tetragonal lattice, or *vice versa*, except under special conditions. The conditions for an exact lattice transformation between high-quartz and keatite phases may be computed from the transformation matrix. The ideal c/a ratio for such a transformation turns out to be close to the actual one. This could be one of the reasons why a reconstructive transformation between high-quartz and keatite phases is possible. A comparison of the lattice constants is listed in Table 4.

Coordinate matrix

The atom movements during the reconstructive transformation may be followed by means of the co-
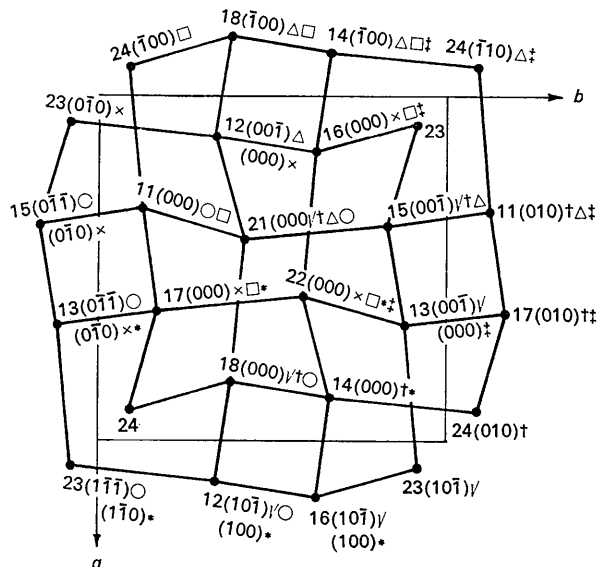
Fig. 3. The projection of LiAlSi₂O₆ keatite phase down the c axis (The eight 7-membered rings are separately marked).

Table 3. *Index transformation between high-quartz and keatite phases of* LiAlSi₂O₆ *composition*

	High-quartz phase				Keatite phase		
hkl	2θ*	*d*	I_1/I_0†	*HKL*	2θ*	*d*	I_1/I_0†
100	19·65°	4·518 Å	11·7	111	19·26°	4·608 Å	8·3
1̄10	19·65	4·518		002̄	19·39	4·578	0·0
101	25·58	3·482	100·0	201	25·55	3·486	100·0
1̄11	25·58	3·482		11̄2	25·65	3·474	19·7
110	34·38	2·609	3·8	220	33·61	2·666	0·2
12̄0	34·38	2·609		11̄3	33·84	2·649	1·9
102	38·51	2·338	0·9	31̄1	39·03	2·308	0·8
1̄12	38·51	2·338		22̄2	39·10	2·304	3·6
200	39·91	2·259	3·8	222	39·10	2·304	
22̄0	39·91	2·259		004	39·36	2·289	1·4
201	43·34	2·088	4·1	312	42·75	2·115	3·2
2̄1	43·34	2·088		11̄4	43·00	2·103	1·3
112	48·24	1·887	19·1	400	48·27	1·885	10·0
12̄2	48·24	1·887		13̄3	48·44	1·879	8·4
202	52·57	1·741	1·4	402	52·49	1·743	0·9
2̄2	52·57	1·741		22̄4	52·70	1·737	0·0
210	53·67	1·708	0·6	331	52·44	1·745	0·0
23̄0	53·67	1·708		1̄15	52·86	1·732	0·1
31̄0	53·67	1·708		224	52·70	1·737	0·0

* Cu-radiation was used.
† The calculated integrated powder intensity was used.

Table 4. *A comparison of lattice constants between high-quartz and keatite phases of* LiAlSi₂O₆ *composition*

	High-quartz solid solution	Keatite solid solution (transformation)	Keatite ss*	High-quartz solid solution (transformation)
a (Å)	5·217	5·298	7·541	7·555
c (Å)	5·464	5·332	9·156	9·036
V (Å³)	128·8	129·6	520·7	515·8
c/a	1·047	1·006	1·214	1·196
Ideal c/a		1·000		1·225

* ss = Solid solution.

ordinate transformation matrix. A successful position transformation depends upon the completion of the following requirements:

(A) It is necessary to provide a common origin for both the high-quartz and the keatite phases. The high-quartz phase has space group $P6_222$ or $P6_422$, while the keatite phase has space group $P4_32_12$ or $P4_12_12$. It is obvious that the space group of the high-quartz does not share a common origin with that of keatite. Thus, an origin transformation has to be derived. The origin transformation may be derived by a method of convergency. This method involves the conversion of 12 T atoms in a keatite unit cell into 3 T atoms in a high-quartz unit cell, where T represents a mixture of Si and Al atoms. The three transformed keatite T atom positions are compared with those of the observed high-quartz data, and the origin transformation $(\frac{1}{4}, \frac{1}{4}, \frac{1}{6})$ is thus obtained. It is worth mentioning here that any change in the selection of the three independent pairs of the equivalent reflections may in turn change the transformation matrix, the pairing of the space group, and the origin transformation, as illustrated in Table 5. This change in selecting the reflection pairs may vary from the inclusion of some or all new pairs to the using of the same three pairs but in different equivalent forms. However, such a change does not affect the corresponding atomic positions related by the transformation matrix, i.e. the same corresponding atomic positions are always reached irrespective of which three

pairs of equivalent reflections are used as long as they are independent.

(B) A proper atom identification system is essential for matching the corresponding atom pair between the two phases, for identifying the loops or rings, and for locating the close neighbors. It is necessary not only to distinguish the symmetry-related equivalent atoms, but also to identify translation-related atom sets. The atom identification system used throughout this paper is as follows: Each atom is identified by two integers and followed by a parenthesis, e.g. 13 (000). The numbers in parentheses describe the translations, e.g. $(1\bar{1}0)$ represents $x+1$, $y-1$, z where $1\cdot0>x,y$ or $z>0\cdot0$. Each atom position x,y,z inside the unit cell is defined as (000). The first integer designates the type of independent atom, e.g. in the keatite phase, 1 and 2 are used for T(1) and T(2), 3 through 5 for O(1) to O(3), and 6 for Li(1). The second integer describes the symmetry-related position, e.g. for a general position of the keatite phase, 1 through 8 are used respectively for x,y,z; $y,x,\bar{z}$; $\bar{x},\bar{y},\frac{1}{2}+z$; $\bar{y},\bar{x},\frac{1}{2}-z$; $\frac{1}{2}-y,\frac{1}{2}+x,\frac{3}{4}+z$; $\frac{1}{2}-x,\frac{1}{2}+y,\frac{3}{4}-z$; $\frac{1}{2}+y,\frac{1}{2}-x,\frac{1}{4}+z$; and $\frac{1}{2}+x,\frac{1}{2}-y,\frac{1}{4}-z$. All the atom positions before and after the transformation, plus the atom displacements during the transformation are listed in Tables 6, 7 and 8.

(C) Some ways have to be designed to identify the bond breakages. Two ways are used in this study. The first one is by taking note of any unusually large atom displacements (see Table 6). Such an atom is usually

Table 5. *Effects of selecting equivalent reflections on transformation matrix, equivalent space group, and origin transformation*

| Equivalent reflections* | | Transformation matrix | Equivalent space group | | Origin |
High-quartz	Keatite	n	Keatite	High-quartz	transformation
hkl	*HKL*	$\frac{1}{2},\frac{1}{2},\frac{1}{2}/\frac{1}{2},\frac{1}{2},-\frac{1}{2}/\frac{1}{2},-\frac{1}{2},0$	$P4_32_12$	$P6_422$	$\frac{1}{4},\frac{1}{4},\frac{1}{6}$
hkl	*HKL̄*	$\frac{1}{2},\frac{1}{2},-\frac{1}{2}/\frac{1}{2},\frac{1}{2},\frac{1}{2}/\frac{1}{2},-\frac{1}{2},0$	$P4_32_12$	$P6_222$	$\frac{1}{4},\frac{1}{4},-\frac{1}{6}$
hkl̄	*HKL*	$\frac{1}{2},\frac{1}{2},\frac{1}{2}/\frac{1}{2},\frac{1}{2},-\frac{1}{2}/-\frac{1}{2},\frac{1}{2},0$	$P4_32_12$	$P6_222$	$\frac{1}{4},\frac{1}{4},-\frac{1}{6}$
hkl	*HK̄L*	$\frac{1}{2},-\frac{1}{2},\frac{1}{2}/\frac{1}{2},-\frac{1}{2},-\frac{1}{2}/\frac{1}{2},\frac{1}{2},0$	$P4_32_12$	$P6_222$	$0,\frac{1}{2},-\frac{1}{4}$
hkl	*H̄KL*	$-\frac{1}{2},\frac{1}{2},\frac{1}{2}/-\frac{1}{2},\frac{1}{2},-\frac{1}{2}/-\frac{1}{2},-\frac{1}{2},0$	$P4_32_12$	$P6_222$	$\frac{1}{2},0,-\frac{1}{6}$

* The equivalent reflections used here are still the three independent pairs mentioned in Table 2, but some different combinations of the equivalent forms are chosen for illustration.

Table 6. T-*atom positions* ($\times 10^3$) *before and after transformation*

High-quartz atom	High-quartz (transformation)			Keatite (obs.)			Atom displacement	Keatite atom
	X	Y	Z	X	Y	Z		
12 (100)	333	167	250	332	122	238	0·353 Å	11 (000)
11 (100)	167	333	750	122	332	762	0·353	12 (000)
11 (210)	667	833	750	668	878	738	0·353	13 (000)
12 (210)	833	667	250	878	668	262	0·353	14 (000)
13 (20$\bar{1}$)	375	875	1000	378	832	988	0·340	15 (000)
13 (10$\bar{1}$)	125	625	500	168	622	512	0·340	16 (000)
13 (100)	625	125	500	622	168	488	0·340	17 (000)
13 (110)	875	375	000	832	378	012	0·340	18 (000)
11 (110)	417	583	250	418	418	000	2·607	21 (000)
12 (200)	583	417	750	582	582	500	2·607	22 (000)
12 (20$\bar{1}$)	083	917	750	082	918	750	0·012	23 (000)
11 (111)	917	083	250	918	082	250	0·012	24 (000)

involved in the bond breakage. The second and easier way is by comparing the close neighbors before and after the transformations.

Discussion of transformation mechanism

The keatite phase of LiAlSi$_2$O$_6$ composition has a unit cell with approximately four times the volume of that of the corresponding high-quartz phase. In order to facilitate the comparison between the two phases, the high-quartz cell is enlarged four times in order to reach a size equivalent to the keatite cell. It was found that the enlarged high-quartz cell whose space group is chosen as $P6_422$ will be exactly correlated to a keatite cell of $P4_32_12$ according to the transformation matrix, if the enlarged high-quartz cell has axes chosen as follows: $2a$ from a to $3a$, $2b$ from 0 to $2b$, and c from 0 to $-c$. Also, all the T atoms in the high-quartz phase are relabeled by the corresponding keatite identification system for the easiness of comparison with the counterparts in the keatite phase. This was done for Tables 9 and 10 and for all the Figures wherever the high-quartz phase was involved.

Change of atom locations

(A) T atoms

By inspecting close neighbors, the two T atoms having the large displacements of 2·607 Å (See Table 6) were confirmed to break the framework tetrahedra linkage of the high-quartz phase. These two T atoms are not neighbors of the other two T atoms having the small displacement of 0·012 Å. But, the remaining

eight T atoms which show medium displacements of 0·340 and 0·353 Å are neighbors of both types of T atoms (see Fig. 4). Because the eight T atoms are lo-
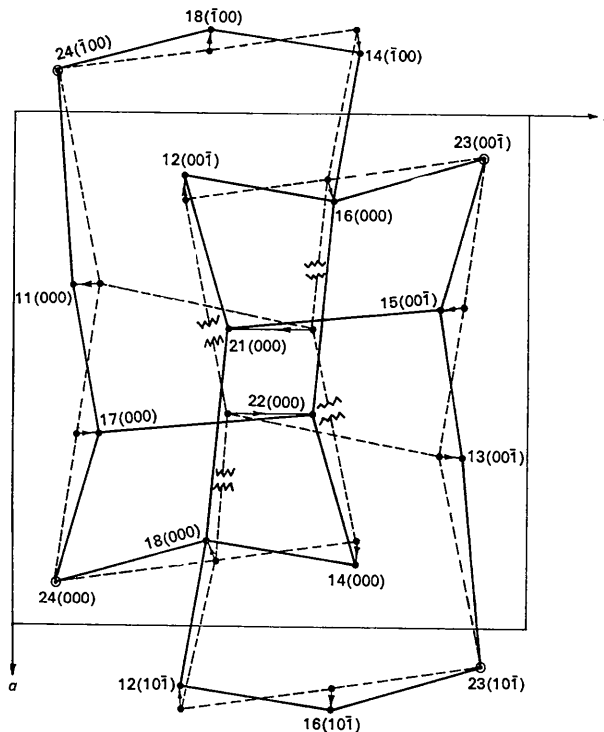
Fig. 4. Displacements of T atoms during the transformation (Heavy lines for keatite and dotted ones for high-quartz phase).

Table 7. *Oxygen-atom positions* ($\times 10^3$) *before and after transformation*

High-quartz atom	High-quartz (transformation)			Keatite (obs.)			Atom displacement	Keatite atom
	X	*Y*	*Z*	*X*	*Y*	*Z*		
21 (100)	446	113	397	443	121	393	0·075 Å	31 (000)
25 (10$\bar{1}$)	113	446	603	121	443	607	0·075	32 (000)
22 (20$\bar{1}$)	554	887	897	557	879	893	0·075	33 (000)
24 (110)	887	554	103	879	557	107	0·075	34 (000)
24 (11$\bar{1}$)	387	1054	103	379	943	143	0·915	35 (000)
21 (10$\bar{1}$)	−054	613	397	057	621	357	0·915	36 (000)
25 (100)	613	−054	603	621	057	643	0·915	37 (000)
22 (200)	1054	387	897	943	379	857	0·915	38 (000)
26 (000)	125	125	294	125	116	299	0·083	41 (000)
23 (1$\bar{1}$0)	125	125	706	116	125	700	0·083	42 (000)
26 (210)	875	875	794	876	884	799	0·083	43 (000)
23 (210)	875	875	206	884	876	201	0·083	44 (000)
25 (11$\bar{1}$)	363	696	103	384	625	049	0·746	45 (000)
22 (10$\bar{1}$)	304	637	397	376	616	451	0·746	46 (000)
24 (100)	637	304	603	616	376	549	0·746	47 (000)
21 (200)	696	363	897	625	384	951	0·746	48 (000)
23 (100)	375	375	206	364	305	146	0·767	51 (000)
26 (100)	375	375	794	305	364	854	0·767	52 (000)
23 (200)	625	625	706	636	695	646	0·767	53 (000)
26 (110)	625	625	294	695	636	354	0·767	54 (000)
21 (20$\bar{1}$)	196	863	893	195	864	896	0·015	55 (000)
24 (10$\bar{1}$)	137	804	603	136	805	604	0·015	56 (000)
22 (100)	804	137	397	805	136	396	0·015	57 (000)
25 (110)	863	196	103	864	195	104	0·015	58 (000)

cated between the two groups of T atoms having large and small displacements, it seems natural for them to have the medium displacements which are just some average between small and large displacements.

(B) Oxygen atoms

The displacements of oxygen atoms during the transformation are closely associated with those of the T atoms, owing to the necessity to maintain a reasonable tetrahedral configuration. As can be seen in Table 7, the 24 oxygen atoms in the enlarged high-quartz cell may be evenly divided into two groups according to their displacements. One group has small displacements of 0·015 to 0·083 Å, while the other has large ones of 0·746 to 0·915 Å. As might be expected, the displacement is large for the eight oxygen atoms attached to the two T atoms with large displacements, and the displacement is small for the eight oxygen atoms bonded to the other two T atoms with small displacements. The remaining eight oxygen atoms are equally divided between small and large displacements, because they are attached to the eight T atoms having medium displacements.

(C) Lithium atoms

There are four lithium atoms distributed over 12 equivalent sites, or $\frac{1}{3}$ Li per site in the enlarged high-quartz cell. The 12 equivalent sites have to be transformed into one eightfold and one fourfold sites, because these are the only two sites available in the keatite phase. But, according to the observed data, the lithium atoms only occupy one eightfold site, *i.e.* four pair-sites in the keatite phase (the keatite structure requires one Li atom per pair-site). Thus, all the lithium atoms at the additional fourfold site have to move toward the eightfold site. Unfortunately, the fourfold site is close only to half of the eightfold site. As a result,

each of the half of the four pair-sites has $\frac{2}{3}$ Li atoms, while each of the other half contains only $\frac{2}{3}$ Li atom instead of the observed value of one Li atom. This dilemma was solved by the following relation: It was found (see Table 8) that out of 12 equivalent sites in the enlarged high-quartz cell, 8 of them transform into the eightfold site with $\frac{1}{3}$ Li each and the final locations in the keatite are reached by making some displacements. The remaining 4 equivalent sites transform into not 4 but also an eightfold site but with only $\frac{1}{6}$ Li each and the same final locations are reached by making somewhat larger displacements. Now, each pair-site contains exactly one Li atom as is shown in the following:

$$2(\tfrac{1}{3}) + 2(\tfrac{1}{6}) = 1\cdot 0$$

Two-thirds of the lithium atoms were found to have large displacements of 2·003, 2·452, or 2·700 Å. They are suspected and later confirmed by the close neighbor approach to be involved in bond breakages. Two out of four Li–O bonds for each involved Li-tetrahedron are broken. The chance for each of the four lithium atoms in the enlarged high-quartz cell to be involved in a bond breakage is 33, 33, 100 or 100%.

Change of (Si,Al)-tetrahedra linkage

In the enlarged high-quartz cell, there are eight 6-membered rings and eight 8-membered rings of (Si,Al)-tetrahedra. During the transformation, all the eight 6-membered rings and four of the 8-membered rings change into eight 5-membered rings and eight 7-membered rings of the keatite phase. The other four 8-membered rings remain unchanged in linkage throughout the transformation.

Since all the 8-membered rings are made up of 6-membered rings, the high-quartz structure can be considered to be made up by the 6-membered rings only.

Table 8. Li-*atom positions* ($\times 10^3$) *before and after transformation*

High-quartz atom*	High-quartz (transformation)			Keatite (obs.)			Atom displacement	Keatite atom†
	X	Y	Z	X	Y	Z		
31 (100)	042	208	500	071	195	501	0·239 Å	61 (000)
32 (100)	208	042	500	195	071	499	0·239	62 (000)
32 (220)	958	792	000	930	805	001	0·239	63 (000)
31 (310)	792	958	1000	805	930	999	0·239	64 (000)
31 (110)	292	458	000	305	571	251	2·452	65 (000)
31 (210)	542	708	500	430	695	249	2·452	66 (000)
32 (210)	708	542	500	695	430	751	2·452	67 (000)
32 (200)	458	292	1000	571	305	749	2·452	68 (000)
33 (10$\bar{1}$)	−125	375	500	071	195	501	2·003	61 (000)
33 (100)	375	−125	500	195	071	499	2·003	62 (000)
33 (220)	1125	625	000	930	805	001	2·003	63 (000)
33 (31$\bar{1}$)	625	1125	1000	805	930	999	2·003	64 (000)
33 (11$\bar{1}$)	125	625	000	305	571	251	2·700	65 (000)
33 (21$\bar{1}$)	375	875	500	430	695	249	2·700	66 (000)
33 (210)	875	375	500	695	430	751	2·700	67 (000)
33 (200)	625	125	1000	571	305	749	2·700	68 (000)

* The site occupancies for the high-quartz phase are $\frac{1}{3}$ Li per site for the first eight sites and $\frac{1}{6}$ Li per site for the remaining eight sites.

† Each keatite site has an occupancy of $\frac{1}{2}$ Li.

Therefore, the transformation is simply a change from 6- into 5- and 7-membered rings. Two 6-membered rings may share either one or two edges. During the transformation, two such neighboring 6-membered rings may change into exactly one 5- and one 7-membered rings. But quite often, two such 6-membered rings may pick up one or two new (Si, Al)-tetrahedra

and at the same time the same number of the original tetrahedra are dropped in order to change into one 5- and one 7-membered rings. The detail of such ring transformation is listed in Table 9 and illustrated in Figs. 5 and 6. One way to describe the transformation mechanism is to follow the breakages of the 6-membered rings. The transformation starts when either one

Table 9. *Change of* (Si, Al)-*tetrahedra linkage from high-quartz to keatite phases*

High-quartz (6-membered rings)	Keatite (5- and 7-membered rings)
A. Two 6-membered rings sharing one common edge	
1. Rearrangement by breaking the common edge	
(*a*) 21–11–17–24–18–14 and 21–15–11–17–24–14 The broken common edge is 21–14	21–11–17—24–18 and 21–15–11–17–24–14–18 The new common edge is 21–18
(*b*) 22–13–15–23–16–12 and 22–17–13–15–23–12 The broken common edge is 22–12	22–13–15–23–16 and 22–17–13–15–23–12–16 The new common edge is 22–16
2. Rearrangement by breaking two adjacent edges, one at each ring, right next to the common edge	
(*a*) 14–18–24–17–11–21 and 16–14–18–24–11–21 The common edge is 11–21 Broken edges are 21–14 and 21–16	14–18–24–17–22 and 16–14–18–24–11–17–22 The common edge is 22–17 New edges are 22–14 and 22–16 The added new T-atom is 22 The dropped old T-atom is 21
(*b*) 12–16–23–15–13–22 and 18–12–16–23–13–22 The common edge is 13–22 Broken edges are 22–12 and 22–18	12–16–23–15–21 and 18–12–16–23–13–15–21 The common edge is 21–15 New edges are 21–12 and 21–18 The added new T-atom is 21 The dropped old T-atom is 22
B. Two 6-membered rings sharing two common edges	
1. Rearrangement by breaking one common edge	
(*a*) 21–11–24–18–14–16 and 21–15–11–24–14–16 Common edges are 21–16 and 14–16 The broken common edge is 21–16	21–11–24–18–12 and 21–15–11–24–14–18–12 Common edges are 21–12 and 18–12 The new edge is 21–12 The added new T-atom is 12 The dropped old T-atom is 16
(*b*) 22–13–23–16–12–18 and 22–17–13–23–12–18 Common edges are 22–18 and 12–18 The broken common edge is 22–18	22–13–23–16–14 and 22–17–13–23–12–16–14 Common edges are 22–14 and 16–14 The new edge is 22–14 The added new T-atom is 14 The dropped old T-atom is 18
2. Rearrangement by breaking two adjacent edges, one at each ring, of one particular common edge	
(*a*) 14–24–17–11–15–15–21 and 16–14–24–11–15–21 Common edges are 21–15 and 11–15 Broken edges are 21–16 and 21–14	14–24–17–13–22 and 16–14–24–11–17–13–22 Common edges are 22–13 and 17–13 New edges are 22–14 and 22–16 Added new T-atoms are 22 and 13 Dropped old T-atoms are 21 and 15
(*b*) 12–23–15–13–17–22 and 18–12–23–13–17–22 Common edges are 22–17 and 13–17 Broken edges are 22–12 and 22–18	12–23–15–11–21 and 18–12–23–13–15–11–21 Common edges are 21–11 and 15–11 New edges are 21–12 and 21–18 Added new T-atoms are 21 and 11 Dropped old T-atoms are 22 and 17

common edge of two such neighboring 6-membered rings is broken or the two adjacent edges, one at each ring, of the particular common edge are broken (see Figs. 5 and 6).

Table 10. *Change of bonding during transformation*

High-quartz T–O–T	Keatite T–O–T	Bonding change Broken T–O	Generated T–O
22–52–12	22–46–16	22–52	22–46
22–48–18	22–54–14	22–48	22–54
22–53–13	22–53–13		
22–47–17	22–47–17		
21–46–16	21–52–12	21–46	21–52
21–54–14	21–48–18	21–54	21–48
21–51–11	21–51–11		
21 45 15	21–45–15		

Another way to visualize the transformation mechanism is to look at all the bond breakages within the enlarged high-quartz cell as a whole. The eight 6-membered rings in this cell are evenly divided into two groups and each group has a common (Si,Al)-tetrahedron. The two common T atoms at the center of each group are 21 (000) and 22 (000) (Fig. 1). Transformation starts when two of the four T–O bonds for each of the two common tetrahedra are broken. Then, each common T atom brings the two remaining oxygen linkages with it and moves a distance of 2·607 Å. Two new T–O bonds are formed for each of the two common T atoms when one T atom joins the two oxygen atoms which are set free by the other T atom. See Table 10 and Fig. 7 for the detail.

During the transformation, only two out of twelve T atoms in the enlarged high-quartz cell are involved in
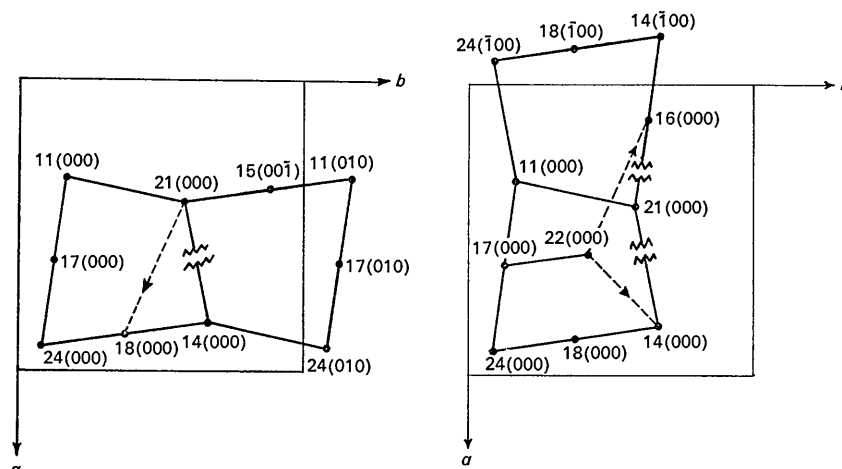
Fig. 5. Illustration of transformation mechanism (I): In the high-quartz projection, two neighboring 6-membered rings sharing one common edge transform into one 5- and one 7-membered rings by breaking the common edge (left) or by breaking the two adjacent edges of the common edge (right) (See Table 9).
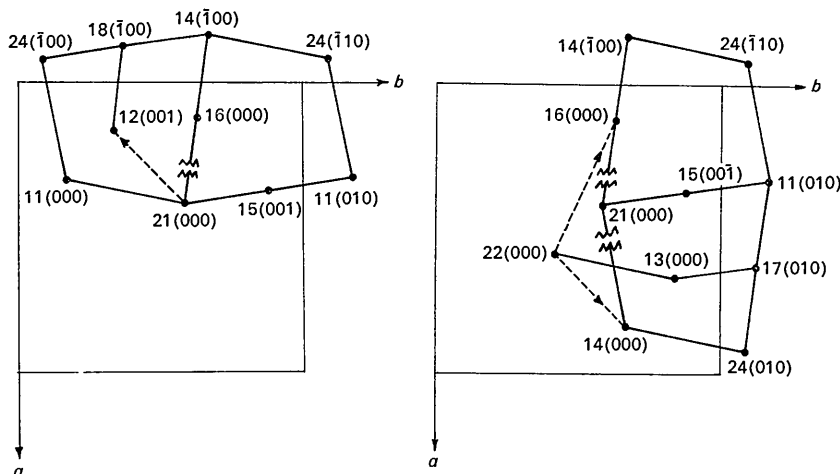
Fig. 6. Illustration of transformation mechanism (II): In the high-quartz projection, two neighboring 6-membered rings sharing two common edges transform into one 5- and one 7-membered rings by breaking one common edge (left) or by breaking the two adjacent edges of the particular common edge (right) (See Table 9).

the bond breakage, and only four out of the forty-eight T–O bonds or four out of twenty-four T–O–T angles are broken. Each 5- or 7-membered ring has only one new T–O bond generated during the transformation.

Change of bond distances and angles

After the transformation, the density decreases from 2·395 to 2·365 g.cm⁻³. This is reflected in a general increase of the bond lengths in the keatite phase (Li & Peacor, 1968; Li, 1968). Also, after the transformation, both the (Si,Al)- and Li-tetrahedra become slightly more distorted, as is shown by a general increase in the range of angles in the keatite phase. During the transformation, the T–O–T angle changes from 151·6° to 143·6°, 150·7° and 154·0°. It was found by this study that the angles of 143·6° and 154·0° are the new T–O–T angles generated during the transformation. However, these two new angles not only show up at the new (Si,Al)-tetrahedra linkage but also appear with the left-over high-quartz linkage of the keatite phase. The remaining T–O–T angle of 150·7° which has the minimum deviation from the original high-quartz angle of 151·6° is the direct descendant from the high-quartz phase.

Reasons for transformation

Some possible reasons for the reconstructive transformation between the high-quartz and the keatite phases were reported (Li, 1970). They will not be repeated here.

The writer would like to express his gratitude to Professor D. R. Peacor and his colleagues, Drs M. A. Conrad, G. M. Muchow, and G. F. Neilson for review-
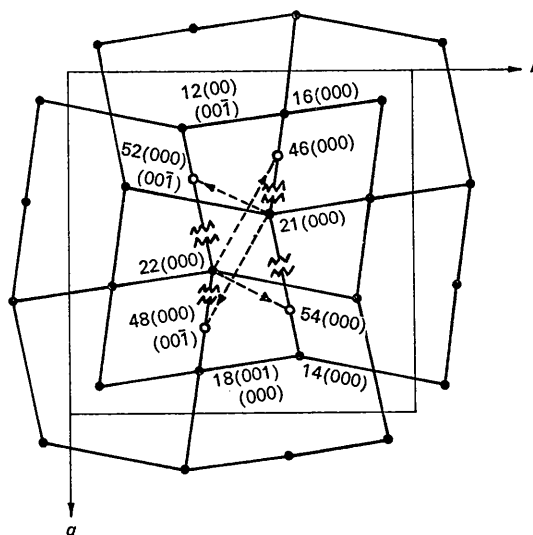
Fig. 7. Illustration of the change of bonding during transformation (open circles designate oxygen locations which are somewhat displaced in this high-quartz projection for sake of clarity).

ing the manuscript. Special thanks are given to Professor Werner Baur for his constructive suggestions in condensing the manuscript.

References

EVANS, D. L. (1969). *Acta Cryst.* A**25**, S 234.
LI, CHI-TANG (1968). *Z. Kristallogr.* **127**, 327.
LI, CHI-TANG (1970). *Z. Kristallogr.* **132**, 118.
LI, CHI-TANG & PEACOR, D. R. (1968). *Z. Kristallogr.* **126**, 46.

Die Strukturen einiger *p*-Halogenphenyl-diphenyl-phosphinchalkogene.
I. *p*-Bromphenyl-diphenyl-phosphinoxid

VON W. DREISSIG UND K. PLIETH

Institut für Kristallographie der Freien Universität, Berlin-Dahlem, Deutschland

p-Bromophenyldiphenylphosphine oxide is monoclinic, space group $P2_1/n$, with lattice constants $a = 16·933$, $b = 14·912$, $c = 6·257$ Å, $\beta = 95·30°$. Three-dimensional intensity data were collected with an automatic 4-circle diffractometer. The structure was determined by Patterson synthesis applying the heavy-atom method. By least-squares refinement, including the 14 H atoms, the *R* value decreased to 6·4%.

Experimente

p-Bromphenyl-diphenyl-phosphinoxid

$$Br-C_6H_4-P-(C_6H_5)_2$$
$$\parallel$$
$$O$$
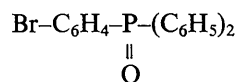
bildet nach Goetz, Nerdel & Wiechtel (1963) farblose Kristalle mit linealförmigem Habitus, die stark zur Verzwillingung neigen. Aus einer 4:1-Lösung von Äthylalkohol und Petroläther konnten nach vielen Kristallisationsversuchen genügend grosse unverzwillingte Kristalle erhalten werden. Die Gitterkon-